Biochemical Pharmacology 83 (2012) 27–36

Contents lists available at SciVerse ScienceDirect

Biochemical Pharmacology

journal homepage: www.elsevier.com/locate/biochempharm

Role of tyrosyl-DNA phosphodiesterase 1 and inter-players in regulation of tumor cell sensitivity to topoisomerase I inhibition

Paola Perego [a,*], Giacomo Cossa [a], Stella Tinelli [a], Elisabetta Corna [a], Nives Carenini [a], Laura Gatti [a], Michelandrea De Cesare [a], Emilio Ciusani [b], Franco Zunino [a], Elena Luison [c], Silvana Canevari [c], Nadia Zaffaroni [a], Giovanni Luca Beretta [a]

[a] Molecular Pharmacology Unit, Dept. Experimental Oncology and Molecular Medicine, Fondazione IRCCS Istituto Nazionale Tumori, via Amadeo 42, 20133 Milan, Italy
[b] Fondazione IRCCS Istituto Neurologico Carlo Besta, via Celoria 11, 20133 Milan, Italy
[c] Molecular Therapies Unit, Dept. Experimental Oncology and Molecular Medicine, Fondazione IRCCS Istituto Nazionale Tumori, via Amadeo 42, 20133 Milan, Italy

ARTICLE INFO

Article history:
Received 29 July 2011
Accepted 19 September 2011
Available online 29 September 2011

Keywords:
Tyrosyl-DNA phosphodiesterase 1
Camptothecin
DNA topoisomerase I
Drug resistance
DNA repair

ABSTRACT

Tyrosyl-DNA phosphodiesterase 1 (TDP1) plays a unique function as it catalyzes the repair of topoisomerase I-mediated DNA damage. Thus, ovarian carcinoma cell lines exhibiting increased TDP1 levels and resistance to the topoisomerase I poisons campthotecins were used to clarify the role of this enzyme. The camptothecin gimatecan was employed as a tool to inhibit topoisomerase I because it produces a persistent damage. The resistant sublines displayed an increased capability to repair drug-induced single-strand breaks and a reduced amount of drug-induced double-strand breaks, which was enhanced following TDP1 silencing. In loss of function studies using U2-OS cells, we found that TDP1 knockdown did not produce a change in sensitivity to camptothecin, whereas co-silencing of other pathways cooperating with TDP1 in cell response to topoisomerase I poisons indicated that XRCC1 and BRCA1 were major regulators of sensitivity. No change in cellular sensitivity was observed when TDP1 was silenced concomitantly to RAD17, which participates in the stabilization of collapsed replication forks. The expression of dominant-negative PARP1 in cells with reduced expression of TDP1 due to a constitutively expressed TDP1 targeting microRNA did not modulate cell sensitivity to camptothecin. Mild resistance to gimatecan was observed in cells over-expressing TDP1, a feature associated with decreased levels of drug-induced single-strand breaks. In conclusion, since TDP1 alone can account for mild levels of camptothecin resistance, repair of topoisomerase I-mediated DNA damage likely occurs through redundant pathways mainly implicating BRCA1 and XRCC1, but not RAD17 and PARP1. These findings may be relevant to define novel therapeutic strategies.

1. Introduction

Topoisomerase I (Topo I) is a nuclear enzyme that plays an essential role in DNA replication, transcription, recombination and repair [1,2]. The enzyme catalyzes changes in the topology of DNA by transiently breaking one strand of DNA with covalent attachment to the 3′ terminus of the nicked DNA leading to the formation of a Topo I covalent complex (i.e., cleavable complex) through a tyrosine hydroxyl group of the enzyme. Topo I is the cellular target of camptothecins (CPTs), which act specifically at the level of the DNA–Topo I complex and, through stabilization of the complex, they stimulate DNA cleavage [1,2]. CPTs are used in the treatment of a variety of human tumors, including ovarian carcinoma [3,4].

In spite of the therapeutic potential of Topo I inhibitors, development of resistance is a major limitation to the success of antitumor therapy with CPTs [5,6]. Since the critical event in the cytotoxic effect of CPTs is the formation of the ternary DNA–Topo I–drug complex, cellular resistance to CPTs can occur by mechanisms reducing the formation of the cleavable complex. Alterations leading to reduced drug–target interaction such as decreased drug accumulation resulting from over-expression of ATP binding cassette transporters [7–11]; mutations of the Topo I

* Corresponding author at: Fondazione IRCCS Istituto Nazionale Tumori, Room 1-62, via Amadeo 42, 20133 Milan, Italy. Tel.: +39 0223902237; fax: +39 0223902692.
E-mail addresses: paola.perego@istitutotumori.mi.it (P. Perego), giacomo.cossa@istitutotumori.mi.it (G. Cossa), stella.tinelli@istitutotumori.mi.it (S. Tinelli), elisabetta.corna@istitutotumori.mi.it (E. Corna), nives.carenini@istitutotumori.mi.it (N. Carenini), laura.gatti@istitutotumori.mi.it (L. Gatti), andrea.decesare@istitutotumori.mi.it (M. De Cesare), eciusani@istituto-besta.it (E. Ciusani), franco.zunino@istitutotumori.mi.it (F. Zunino), elena.luison@istitutotumori.mi.it (E. Luison), silvana.canevari@istitutotumori.mi.it (S. Canevari), nadia.zaffaroni@istitutotumori.mi.it (N. Zaffaroni), giovanni.beretta@istitutotumori.mi.it (G.L. Beretta).

0006-2952/$ – see front matter © 2011 Elsevier Inc. All rights reserved.
doi:10.1016/j.bcp.2011.09.021

gene [6,12–14]; increased Topo I degradation through ubiquitination or sumoylation have been described in cells selected *in vitro* for resistance to CPTs [15,16]. CPT-resistant cells have been shown to exhibit increased expression of anti-apoptotic proteins [17]. Increased repair of CPT-induced lesions has been reported in CPT-resistant cells. For example, enhanced nucleotide excision repair activity was found in breast cancer cells selected for resistance to CPT [18]; CPT-resistant cell lines exhibit increased XRCC1 levels and transfection of XRCC1 confers CPT resistance [19]. Overexpression of tyrosyl-DNA phosphodiesterase 1 (TDP1) in human cells through transfection has also been associated with decreased damage following exposure to high concentration of CPT [20]. A fraction of the TDP1 enzyme localizes to the mitochondria and acts in repair of mitochondrial DNA [21]. Recently, a human 5′-tyrosyl DNA phosphodiesterase (TTRAP/TDP2) that can cleave 5′-phosphotyrosyl bonds has been implicated in cellular resistance to topoisomerase poisons [22,23].

The 7-substituted lipophilic camptothecin derivative gimatecan – currently undergoing Phase II clinical evaluation – appears a promising drug for the treatment of solid tumors [4]. Cellular studies documented a high growth-inhibitory potency in several human tumor cell lines and the capability to overcome multidrug resistance mediated by different transporters [24–26]. Preclinical evaluation of the antitumor efficacy in human tumor xenografts indicated potent antitumor activity and improved pharmacological profile as compared to topotecan (TPT) [25]. Moreover, among CPTs, gimatecan is a good experimental tool because it produces Topo I cleavable complexes more stable than those formed by other CPTs [24]. Thus, in the present study, we examined the role of TDP1, an enzyme implicated in the repair of strand breaks arising from abortive Topo I complexes, and its putative inter-players in modulating sensitivity to CPTs taking advantage of ovarian carcinoma cell lines resistant to gimatecan generated in our laboratory, exhibiting enhanced TDP1 levels.

2. Materials and methods

2.1. Drugs

Gimatecan (7-terbutoxyiminomethylcamptothecin) [24], SN38, NSC 120686 and NSC 128609 (Sigma–Aldrich Discovery CPR, Milan, Italy) were dissolved in DMSO and diluted in water; TPT and doxorubicin were dissolved in water; etoposide (Vepesid, Bristol-Myers Squibb, Roma, Italy) was dissolved in ethanol and diluted in culture medium.

2.2. Cell lines and growth conditions

The human ovarian carcinoma IGROV-1 cell line [27], the gimatecan-resistant IGROV-1CPT/L and IGROV-1CPT/H sublines, cultured in RPMI-1640 medium, and the human osteosarcoma U2-OS cell line (ATCC), grown in Mc Coy's 5A medium were used. Medium was supplemented with 10% foetal calf serum. Resistant sublines were generated by chronic exposure to increasing gimatecan concentrations starting from 0.011 up to 0.2 μM. Such sublines were designated as IGROV-1CPT/L and IGROV-1CPT/H according to their lower (L) and higher (H) degree of resistance obtained in comparison to parental cells. The phenotype of the studied resistant variants was stable at least for 6 months when cells were grown in the absence of drug. Resistant cells were routinely cultured in the absence of gimatecan. The growth characteristics of sensitive and resistant cells were similar. Polyclonal populations of cells stably transfected with the TDP1 containing vector (U2-OS/TDP1) or empty vector (U2-OS/e) were grown in the presence of 400 μg/ml G418 (Calbiochem Inalco, Milan, Italy). U2-OS cells stably expressing miRNAs were cultured in the presence of blasticidin (2.5 μg/ml, Invitrogen, San Giuliano Milanese, Italy).

2.2.1. Cell sensitivity to drugs

The cell sensitivity to antitumor agents was measured by using the growth-inhibition assay based on cell counting or the sulforhodamine B assay (SRB) [28]. For the former assay, cells were seeded in duplicates into 6-well plates and exposed to drug 24 h later. After 1 h of drug incubation, the medium was replaced with fresh medium. Cells were harvested 72 h later for counting with a cell counter. For the SRB assay, cells were seeded in 96-well plates and, 24 h later, they were treated with drugs for 48 or 72 h. IC_{50} is defined as the drug concentration producing 50% decrease of cell growth/absorbance. For each assay, at least three independent experiments were performed.

2.3. Topo I activity in nuclear extracts

Cells (5×10^6) were harvested after trypsinization, washed with PBS, and resuspended in 5 ml of nuclear buffer [1 mM KH_2PO_4 (pH 6.4), 100 mM NaCl, 5 mM $MgCl_2$, 1 mM EGTA, 10 mM 2-mercaptoethanol, 10% (vol/vol) glycerol]. After addition of 45 ml of nuclear buffer containing 0.35% (vol/vol) Triton X-100 and 0.5 mM PMSF, the cell suspension was kept on ice for 30 min. The nuclei were collected by centrifugation at $1000 \times g$ for 10 min, washed once with Triton X-100-free nuclear buffer and then incubated for 1 h at 4 °C in lysis buffer [5 mM KH_2PO_4 (pH 7.0), 100 mM NaCl, 0.5 mM EGTA, 10 mM 2-mercaptoetanol, 10% (vol/vol) glycerol, 10 mM $NaHSO_3$] containing 0.35 M NaCl in gentle rotation. The lysate was centrifuged at $12{,}000 \times g$ for 15 min and the protein concentration was determined using the BioRad Protein Concentration Assay (Bio-Rad Laboratories Srl, Segrate, Italy). Equal amounts of the nuclear protein extract for each cell line were immediately assayed for Topo I activity. The activity of Topo I was determined by measuring the relaxation of supercoiled pBR322 DNA (Invitrogen). The reaction mixture (final volume 20 μl) containing 20 mM Tris–HCl (pH 8.0), 10 mM $MgCl_2$, 0.1 mM EDTA, 0.5 mg/ml BSA, 150 mM NaCl, and 250 ng of pBR322, and different dilutions of nuclear extract was incubated at 37 °C for 30 min. The reaction was stopped by adding 1% SDS, 0.3 mg/ml proteinase K and incubating for 45 min at 42 °C. The samples were loaded on 1% agarose gel in TBE buffer (0.089 M Tris base, 0.089 M boric acid, and 0.002 M EDTA) and run over night at 40 V. After staining with 0.5 mg/ml ethidium bromide, the gels were photographed under UV light.

2.4. DNA sequence analysis of TOP1 and TDP1

The DNA sequence of TOP1 was analysed by RT-PCR. Total cellular RNA was isolated by using a commercially available kit (Talent, Trieste, Italy). Two micrograms of RNA was reverse transcribed into cDNA with the use of oligo-(dt) primers and Moloney murine leukaemia virus reverse transcriptase (Invitrogen). The entire TOP1 transcripts were amplified in two parts using 2 pairs of primers. The first pair of primes (5′-atgagtggggaccacctccacaa-3′/5′-ttcattagtcatttcctttctccagt-3′) gave a fragment of 867 bp, the second pair (5′-aatgctcgaccatgaatatactacc-3′/5′-taaaactcatagtcttcatcagcc-3′) amplified a DNA fragment of 1512 bp. The TDP1 transcripts were amplified using appropriate primers (5′-atgtctcaggaaggcgattatgggagg-3′/5′-tcaggagggcacccacatgttccc-3′). PCR conditions were as follows: 95 °C, 9 min for 1 cycle; 95 °C, 1 min, 52 °C for TOP1/62 °C for TDP1, 1 min, 72 °C, 1 min for 30 cycles followed by 10 min extension at 72 °C. The amplification products were purified on 1% agarose gel. Sequence analysis was performed by using the indicated primers and others

annealing inside the amplification products. The sequences of such primers will be made available upon request.

2.5. Alkaline elution

Single Strand Breaks (SSBs) and Double Strand Breaks (DSBs) were determined by the alkaline elution method [29]. Briefly, cellular DNA was labeled with 0.08 μCi/ml 2[^{14}C] thymidine for 24 h, and the nucleoside-labeled precursor was removed 24 h before drug exposure. Cells were exposed to gimatecan for 1 h and processed immediately or incubated for 1 h in drug-free medium. Cells were layered on 2 μM pore polycarbonate filters, lysed with a solution containing 2% SDS, 0.1 M glycine, 25 mM disodium EDTA (pH 10 for SSBs, pH 9.6 for DSBs) and 0.5 mg/ml proteinase K and the DNA eluted with a solution containing 0.1% SDS, 20 mM EDTA acid form adjusted to pH 12.15 (for SSBs) or 9.6 (for DSBs) with tetrapropylammonium hydroxide. During the 15 h elution, fractions were collected and radioactivity was measured by liquid scintillation. Three independent experiments were performed for each tested condition.

2.6. Immunofluorescence staining of phosphorylated H2AX and TDP1

The phosphorylated H2AX staining was performed as previously described [29]. Cells were seeded in 24-well plates containing coverslips. After 24 h, they were treated as indicated and then fixed in 2% paraformaldehyde in PBS for 5 min. After washing in PBS, cells were permeabilized in cold methanol (−20 °C) for 20 min and incubated in PBS containing 1% bovine serum albumin and 0.1% Tween-20 for 15 min. The coverslips were then incubated at room temperature for 1 h with a 1:4000 dilution of an anti-phospho-Ser^{139} H2AX antibody (clone JBW301, Upstate Biotechnology Inc., Lake Placid, NY, USA) and thereafter with an AlexaFluor 594 (or 488)-conjugated goat anti-mouse antibody (Molecular Probes – Invitrogen) for 1 h. After washes in PBS, samples were counterstained with Hoechst 33342 (2 mg/ml, Sigma–Aldrich Inc., Milan, Italy) for 2 min and mounted with Mowiol. Images were collected using a fluorescence microscope and DSB-associated nuclear foci were counted on duplicate slides from three independent experiments. For TDP1 immunofluorescence, cells were seeded in 24-well plates containing coverslips, and 24 h later they were treated as indicated and processed as described above. The primary antibody used (1:50 dilution) was a purified rabbit polyclonal antibody (ProteinTech Group Inc., Manchester, UK). The AlexaFluor 594 (or 488)-conjugated goat anti-mouse antibodies (Molecular Probes, Eugene, OR) were employed as secondary antibodies.

2.7. Western blot analysis

Western blot analysis was carried out as described previously [30]. After lysis, samples were fractionated by SDS-PAGE and blotted on nitrocellulose sheets. Blots were pre-blocked in PBS containing 5% (w/v) dried non fat milk and then incubated overnight at 4 °C with antibodies against Topo I (1:500, Becton Dickinson Pharmingen), TDP1 (1:1000; Abcam, Cambridge, UK), TDP2 (Bethyl Laboratory, Montgomery, USA), RAD17 (1:1000; Santa Cruz Biotech Inc., Santa Cruz, CA, USA), XRCC1 (1:1000; Neomarkers, Bio-Optica, Milan, Italy), BRCA1 (Santa Cruz Biotech Inc.), BRCA2 (Oncogene Research Products La Jolla, CA), PARP1 (Upstate biotechnology). Anti-actin and anti-vinculin antibodies (Sigma–Aldrich) were used as control for loading. Antibody binding to blots was detected by chemiluminescence (GE Healthcare, Milan, Italy). For all Western blot analyses at least three independent experiments were performed.

2.8. Small-interfering RNA duplexes and transfections

Non overlapping small-interfering RNA (siRNA) duplexes (Stealth^{TM}, Invitrogen) targeting different regions of TDP1 mRNA were used. Two of them and the corresponding scrambled sequences were designed using a web available program: siRNA-A (5′-CCACCUUUCCUGUGCCAUAUGAUUU-3′; scrambled-A: 5′-CCAUUCUUCUGCGACAUGUACCUUU-3′) and siRNA-B (5′-GGACGCUUGUUUCUUCAGCUCAGUU-3′; scrambled-B: 5′-GGAGUUCCUUUACUUCUCGAGCGUU-3′). A pre-designed siRNA was also employed (Select siRNA–siRNA C – and Stealth RNAi negative control medium GC – control-siRNA C). In addition, a pool of siRNA obtained from Dharmacon (Celbio Srl., Milan, Italy) was also used to confirm the results. In all cases, delivery of siRNAs was obtained using liposome-based techniques. Preliminary experiments were performed to define optimal transfection conditions, i.e., vehicle, siRNA concentrations (10–100 nM for U2-OS, and 30–300 nM for IGROV-1 CPT/L), exposure and harvesting times. The efficiency of down-regulation of target expression was then monitored 2 days after transfection and at cell harvesting by Real-time PCR and Western blotting. For detection of nuclear foci, cells were seeded in 24-well plates containing coverslips, and transfected 24 h later for 4 h in serum-free medium with specific siRNAs or control siRNAs using Lipofectamine2000 (Invitrogen). At the end of transfection, medium was replaced with fresh medium and, 48 h later, cells were incubated for 1 h with gimatecan. Nuclear foci were monitored at the end of treatment. Three independent experiments were performed with duplicate samples, and in each experiment we monitored the decrease of TDP1 before drug treatment and at the end of the experiment by Real-time PCR and/or Western blotting. When analysing cell sensitivity to drug in U2-OS cells transfected with siRNA against TDP1 alone (siRNA A, 100 nM) or combined with a siRNA directed to RAD17 (50 nM, 5′-GCCGCCAAACUCAGCUAUUGCCAUA-3′; scrambled 5′-GCCAAACACUCAUCGCGUUCCGAUA-3′) or to XRCC1 (pool XRCC1 siRNAs and non targeting pool from Dharmacon) 24 h after a 4 h transfection, cells were harvested, seeded in 6-well plates and treated 24 h later for 1 h as described above. Cells were harvested 72 h later for cell counting. Alternatively, when using the SRB assay, cells were seeded in 96-well plates and treated for 48 h. In some cases, cells were seeded in 25 cm^2 flasks and 48 h after transfection they were exposed to drug and then processed for the alkaline comet assay.

2.9. Real-time PCR

RNA extraction, and digestion with DNase were carried out with the RNAqueous®-4PCR Kit (Ambion Europe Ltd., Huntingdon, UK), according to the manufacturer's instructions. RNA purity and integrity were assessed with denaturing gel electrophoresis and the RNA was quantified spectrophotometrically and then stored at −80 °C. cDNA synthesis was performed with the High-Capacity cDNA Reverse Transcription Kit (Applied Biosystems, Monza, Italy) with a Master Mix containing 2.5 U/μl of MultiScribe Reverse Transcriptase and 1 μg of total RNA. The reaction mixture was incubated at 25 °C for 10 min, followed by 120 min at 37 °C and then by heat inactivation of the enzyme at 85 °C for 5 s. The PCR reaction was carried out in a volume of 20 μl containing single-stranded cDNA (5 μl), TaqMan Universal PCR Master Mix (Applied Biosystems, 10 μl), specific TaqMan gene expression assay (1 μl) in nuclease-free water. The reactions were performed using the ABI 7900HT instrument (Applied Biosystems). The relative levels of templates in samples were determined through Relative Quantitation (RQ) using Comparative C_T ($\Delta\Delta C_T$) assay configuration. The GAPDH gene was used as endogenous control. Data analysis was performed with SDS (Sequence Detection Systems) 2.2.2 software (Applied Biosystems).

2.10. Generation of cells expressing TDP1 tailored microRNAs

The U2-OS cells were transfected with a plasmid (pcDNA6.2-GW/Em-GFP, Invitrogen) which allows the expression of miRNA sequences using RNA polymerase II (Pol II) promoters, thus generating an expression clone containing a double-strand oligonucleotide encoding a pre-miRNA sequence. For each miRNA, two single-stranded DNA oligonucleotides were designed using the web-available RNAi designer tool (Invitrogen). The BLOCK-iT Pol II miR RNAi expression vector kit (Invitrogen) was employed for cloning. Briefly, equal amounts of the purified oligonucleotides were annealed and ligated into the pcDNA6.2-GW/Em-GFP vector that was used to transform *Escherichia coli* competent cells. Positive transformants were sequenced to confirm the sequence of the double-strand insert. The plasmids were transfected into U2-OS cells using Lipofectamine 2000 as described above, and were selected and maintained in culture using blasticidin (2.5 μg/ml). A plasmid containing a sequence lacking a target in vertebrates was used as control plasmid (pcDNA6.2-GW/EmGFP-miR-neg control). As the expression vector contains the Emerald Green Fluorescent Protein (EmGFP), cells expressing the miRNA were tracked and sorted using a flow cytometer (FAC-Star Plus, Becton Dickinson, Buccinasco, Italy). The phenotype of the sorted transfectants was checked in Real-time PCR and Western blot experiments. The U2-OS sorted cells which express miRNA directed to TDP1 were used to knock down BRCA1 mRNA by using small-interfering RNA (pool BRCA1 siRNAs and non targeting pool from Thermo Scientific) for 48 h after a 4 h transfection as reported above. The U2-OS cells expressing miRNA directed to TDP1 were also used to transfect pDEST12.2 vector containing cDNA coding for the DNA binding domain (the first 1127 base pairs [S2]) of PARP1 using Lipofectamine2000 (Invitrogen), according to the manufacturer's protocol. Stably transfected cell populations were selected using 400 μg/ml G418 (Calbiochem Inalco). The vector was prepared using the Gateway cloning technology (Invitrogen), employing the RNA of IGROV-1 cells as a template. The obtained expression vector was checked by sequencing the insert.

2.11. Generation of TDP1 over-expressing cells

The U2-OS cells were transfected with the pDEST12.2 vector containing the full-length cDNA of TDP1 using Lipofectamine2000 (Invitrogen), according to the manufacturer's protocol. Stably transfected cell populations were selected using 400 μg/ml G418 (Calbiochem Inalco). The vector was prepared using the Gateway cloning technology (Invitrogen), employing the RNA of IGROV-1 CPT/H cells as a template and primers flanked by attB recombination sites. The obtained expression vector was checked by sequencing the full-length insert.

2.12. Statistical analysis

Statistical analysis was performed using the GraphPad Prism™ software (GraphPad Software, San Diego, CA). Analysis of variance was used to analyse data from growth inhibition assays. A non parametric test (Kruskal–Wallis test) was employed for analysis of comet assay results.

3. Results

3.1. Phenotype of camptothecin-resistant ovarian carcinoma cells

The two human ovarian carcinoma cell sublines, IGROV-1CPT/H and IGROV-1CPT/L, selected by exposure of the ovarian IGROV-1 cell line to gimatecan were resistant to various CPTs and cross-resistant to the Topo II inhibitors doxorubicin and etoposide (Table 1). Although decreased levels of Topo I have been associated with reduced cell sensitivity to CPTs [6], Topo I expression was not markedly reduced in resistant cells (Fig. 1A). The analysis of Topo I activity by DNA relaxation assay indicated a measurable reduction – although not marked – in enzymatic activity, especially for IGROV-1CPT/H cells (Fig. 1B). Sequencing of the coding sequence of the TOP1 gene using the cDNA as a template excluded that expression of a mutant form of the enzyme could account for resistance (data not shown). A moderate increase of ABCC2/MRP2 levels was found in the resistant sublines (Fig. S1) which, however, did not display decreased gimatecan accumulation (Table S1). *In vivo* studies indicated that although less quickly than parental cells, both resistant sublines could generate tumors in nude mice, but with different growth kinetics (Fig. S2A). Gimatecan exhibited moderate activity against IGROV-1CPT/L cells (Fig. S2B). In fact, 12 days after the end of treatment in IGROV-1CPT/L tumors a TVI of 62% was achieved ($P < 0.05$), whereas in IGROV-1 tumors TVI was 84%.

As shown by the alkaline elution assay, the resistant sublines displayed an increased capability to repair gimatecan-induced SSBs. One hour exposure to 0.1 μM gimatecan produced high levels of SSBs in drug-sensitive and -resistant cells, but both IGROV-1CPT/H and IGROV-1CPT/L sublines displayed reduced levels of SSBs 1 h after gimatecan removal, as compared to parental cells (Fig. 1C). A reduced amount of DSBs was also found in the resistant variants after exposure to 0.3 μM gimatecan (Fig. 1D). Immunofluorescence staining of phosphorylated H2AX histone at the DNA damage sites, indicated the induction of a higher amount of γH2AX-associated foci in the IGROV-1 cell line exposed to 0.1 μM gimatecan for 1 h, thereby supporting the presence of higher levels of DSBs than in the resistant variants (Fig. 1E). Based on the function of TDP1, which binds SSBs and hydrolyzes the phosphodiesteric bond between the Topo I tyrosine 723 and the broken DNA strand [31,32], we determined TDP1 expression in the

Table 1
Cell sensitivity of IGROV-1, IGROV-1CPT/L and IGROV-1CPT/H cells to DNA topoisomerase I and II inhibitors and to TDP1 inhibitors.[a]

Drug	IC_{50} (μM)[b]		
	IGROV-1	IGROV-1CPT/L	IGROV-1CPT/H
Gimatecan	0.0313 ± 0.005	0.18 ± 0.05 (5.7)[c]	0.21 ± 0.07(6.7)[c]
Topotecan	0.78 ± 0.3	14.0 ± 1.1 (17.9)[c]	8.4 ± 2.0 (10.8)[c]
SN38	0.18 ± 0.03	1.26 ± 0.05 (7.0)[c]	0.75 ± 0.3 (4.2)[c]
Doxorubicin	1.05 ± 0.25	3.95 ± 0.5 (3.8)[c]	3.7 ± 0.7 (3.5)[c]
Etoposide	10.7 ± 1.9	15.85 ± 2.3 (1.5)[c]	20.75 ± 0.75 (1.9)[c]
NSC120686	9.63 ± 2.9	19.83 ± 5.6 (2)[c]	17.5 ± 3.5 (1.8)[c]
NSC128609	6.8 ± 1.6	19.5 ± 0.86 (2.8)[c]	17.83 ± 1.04 (2.6)[c]

[a] Cell sensitivity to drug was assessed by growth-inhibition assay. 24 h after seeding, cells were exposed to topoisomerase I and II (for 1 h) or TDP1 inhibitors and counted 72 h later.
[b] IC_{50}, drug concentration inhibiting growth by 50%.
[c] RI, resistance index; ratio between IC_{50} values of resistant and sensitive cells.

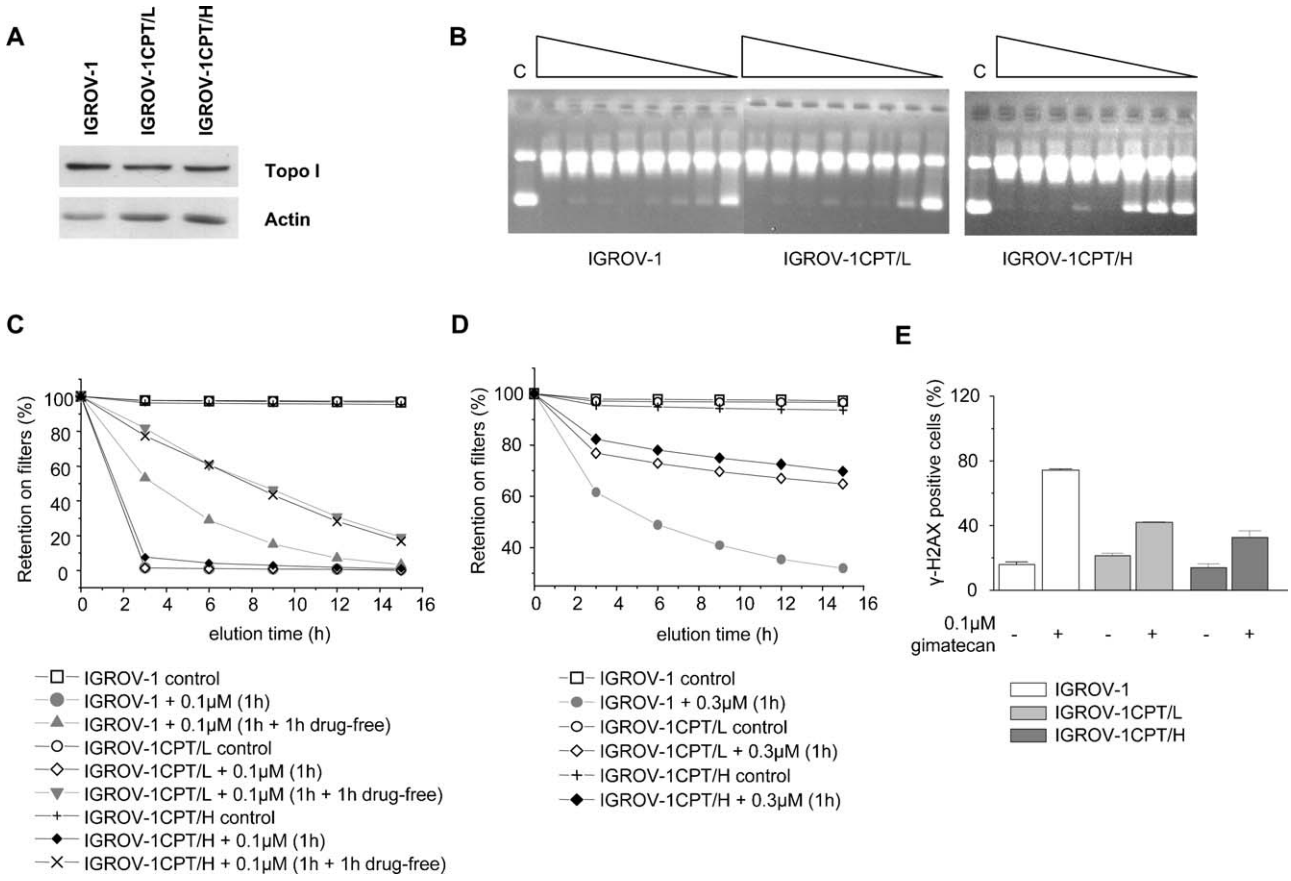

Fig. 1. DNA topoisomerase I protein levels and activity and analysis of DNA damage induced by gimatecan in IGROV-1 and in the two gimatecan-resistant sublines IGROV-1CPT/L and IGROV-1CPT/H. (A) Western blot analysis of lysates prepared from exponentially growing cells. Control loading is shown by β-actin. (B) Activity of Topo I as assessed by the relaxation of supercoiled pBR322 DNA. Different dilutions of nuclear extracts were incubated with 250 ng DNA. C, control – DNA incubated in the absence of nuclear extract. (C) Gimatecan-induced single-strand breaks as measured by alkaline elution following 1 h exposure to equimolar drug concentrations (0.1 μM) and 1 h incubation in drug-free medium. Values are from a representative experiment. (D) Gimatecan-induced double-strand breaks as measured by alkaline elution following 1 h exposure to equimolar drug concentrations (0.3 μM). Values are from a representative experiment. (E) Immunofluorescence staining of phosphorylated γH2AX in cells exposed to 0.1 μM gimatecan for 1 h (indicated as +). Control, refers to untreated cells. Values are the mean (±SD) of 3 independent experiments.

cell systems (Fig. 2A). TDP1 levels were increased in both resistant variants, whereas levels of TDP2, recently proposed to act in concert with TDP1 in DNA repair, were not different (Fig. 2A). XRCC1 levels were not altered (Fig. S3). The IGROV-1CPT/H and IGROV-1CPT/L sublines displayed reduced sensitivity to the TDP1 inhibitors NSC 120686 and NSC 128609 [33] with respect to the parental cells (Table 1). To establish whether TDP1 was involved in resistance to Topo I poisons, we used a RNA interference approach to inhibit its expression. Three non-overlapping siRNAs targeting different regions of TDP1 sequence were employed in the U2-OS cell line, in which a high transfection efficiency can be obtained, thereby providing optimal conditions for assessing the effect of the siRNAs. Under our experimental conditions, all the used RNA duplexes were effective in TDP1 silencing (data not shown). Since the siRNA A exhibited the most marked effect (Fig. 2B), it was chosen for experiments in ovarian cancer cells. Transfection of the siRNA A duplexes targeting TDP1 in the IGROV-1CPT/L resistant subline slightly reduced TDP1 protein level (Fig. 2B) that resulted in a modest increased amount of gimatecan-induced DSB as assessed by γH2AX staining. In IGROV-1 CPT/L, gimatecan-induced nuclear foci were higher in TDP1 siRNA-transfected cells (percent of positive cells: 41.0 ± 8.8) than in scrambled siRNA transfected cells (percent of positive cells: 28.7 ± 8.8). A different model system was chosen to clarify the role of TDP1 because the parental IGROV-1 cells are difficult to transfect under several different experimental conditions (data not shown); also, multiple alterations were found to be associated with the drug-resistant phenotype of ovarian carcinoma cells (e.g., altered levels of apoptotic proteins, data not shown) and such features were considered likely to mask the significance of TDP1 in cell response to Topo I inhibition.

3.2. Effect of knockdown of TDP1 on cell sensitivity to CPT

As shown in Fig. 2C, knockdown of TDP1 in U2-OS cells did not increase sensitivity to gimatecan; in fact, no difference between IC_{50} of siRNA A (0.107 ± 0.02 μM) and of control-siRNA transfected cells (0.092 ± 0.01 μM) was documented using growth-inhibition assays. Similar results were obtained using a pool of siRNA (data not shown). To establish a cell model constitutively down-regulating the levels of TDP1, we used web-available tools to design two exogenous miRNAs directed to TDP1 and the miRNAs were cloned into an expression plasmid under the control of a Pol II promoter. The used vector allows to monitor the expression of the cloned miRNA because of co-expression of the Emerald GFP. Thus, after stable transfection, Emerald GFP positive cells were sorted to enrich the transfected cell population for TDP1 miRNAs expressing cells (Fig. 2D). Real-time PCR analysis of TDP1 transcript indicated that only miRNA A transfected cells significantly down-regulated TDP1 (i.e., around 70% decrease in level *versus* control miRNA cells; data not shown). The observed decrease resulted in a marked protein down-regulation (Fig. 2E). However, the cell sensitivity to gimatecan of U2-OS cells transfected with the EmeraldGFP-tagged microRNA efficiently targeting TDP1

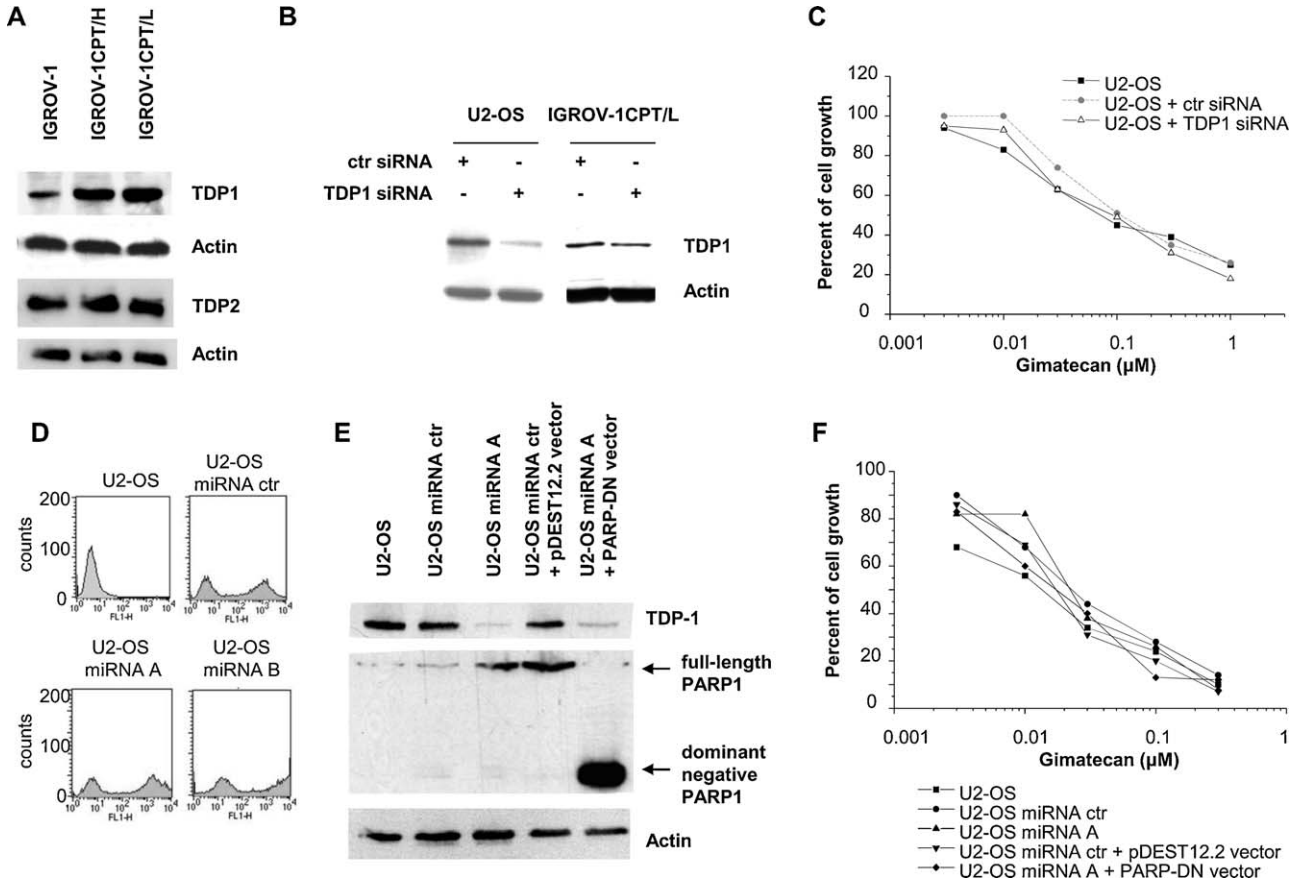

Fig. 2. Western blot analysis of TDP1 and TDP2 levels in IGROV-1, IGROV-1CPT/L and IGROV-1CPT/H and TDP1 and PARP1 loss of function studies in U2-OS cells. (A) Levels of TDP1 and TDP2 in IGROV-1, IGROV-1CPT/L and IGROV-1CPT/H cells. Control loading is shown by β-actin. (B) Levels of TDP1 in U2-OS and IGROV-1CPT/L cells treated with siRNA A. Twenty-four h after seeding cells were transfected for 4 h with 100 nM of the indicated TDP1 targeting siRNA or control siRNA and 48 h after the end of transfection cells were harvested for Western blot analysis. Control loading is shown by β-actin. (C) Cell sensitivity to gimatecan of cells transfected as indicated above measured 72 h after 1 h drug exposure using growth inhibition assay. (D) Flow cytometry analysis of U2-OS cells and polyclonal populations of TDP1 and control miRNAs transfected cells. The cell populations with high fluorescence (FL1 > 10^2) were sorted. (E) Western blot analysis of levels of TDP1 and PARP1 dominant negative in U2-OS cells transfected with miRNA directed to TDP1 and pDEST12.2-PARP-DN. β-Actin was used as control loading. (F) Cell sensitivity to gimatecan of cells transfected as indicated in (D). Standard deviation is less than 5% for each point.

mRNA did not significantly differ from that of control miRNA transfected cells (Fig. 2F).

3.3. Effect of knocking down TDP1 in cells expressing a dominant negative form of PARP1

Since PARP1 is a repair enzyme which binds SSBs and DSBs and may be implicated in targeting a base excision repair complex to sites of Topo I-mediated damage [34], we examined the effect of TDP1 silencing in U2-OS cells overexpressing a dominant-negative form of PARP1 corresponding to the DNA binding domain of the enzyme (Fig. 2E) [35]. Although an optimal expression of PARP1 dominant negative was obtained after transfection of U2-OS cells expressing the TDP1 targeting miRNA, no change in sensitivity to gimatecan was observed (Table S2, Fig. 2F).

3.4. Effect of co-silencing of TDP1 and the checkpoint control gene RAD17

Since studies performed in fission yeast have shown that TDP1 *per se* cannot regulate sensitivity to CPTs, but hypersensitivity to CPT following TDP1 inactivation is obtained in a checkpoint-deficient background (*Rad9*$^{-/-}$ [36]), we examined the effect of simultaneous knocking-down of TDP1 and RAD17. This latter gene was chosen because of its pivotal role in checkpoint response in human cells, in the absence of a well-defined homologue of Rad9. No significant increase in cell sensitivity was observed with simultaneous silencing of TDP1 and RAD17 (Fig. 3B). In fact, in these cells the IC_{50} value after 1 h gimatecan exposure was 0.078 ± 0.003 μM, whereas the values of Rad17 siRNA-, TDP1 siRNA-, and control siRNA-transfected cells were 0.109 ± 0.01 μM, 0.094 ± 0.008 μM and 0.103 ± 0.004 μM (Fig. 3B). Thus, cooperation between TDP1-dependent repair and RAD17-mediated checkpoint response may not be critical in repair of Topo I-mediated DNA damage.

3.5. Effect of co-silencing of TDP1 and possible inter-players

Since the concomitant inactivation of TDP1 and RAD17 or PARP1 did not change sensitivity to Topo I inhibition (Fig. 2E and F, Fig. 3A and B, Table S2), we examined other possible inter-players of TDP1. A putative key regulator of TDP1-mediated repair is XRCC1, an inter-player of the Base Excision Repair repair complex and a direct interactor of TDP1 [19]. Simultaneous knocking-down of TDP1 and XRCC1 in U2-OS cells resulted in increased sensitivity to gimatecan as compared with cells transfected with control siRNA (Fig. 3C and D). The observed sensitization was similar to that found in cells in which only XRCC1 was knocked down (control siRNA 0.064 ± 0.0003 μM, XRCC1 siRNA 0.0071 ± 0.0002 μM, TDP1 siRNA 0.029 ± 0.001 μM and XRCC1/TDP1 siRNA 0.0059 ± 0.0004 μM).

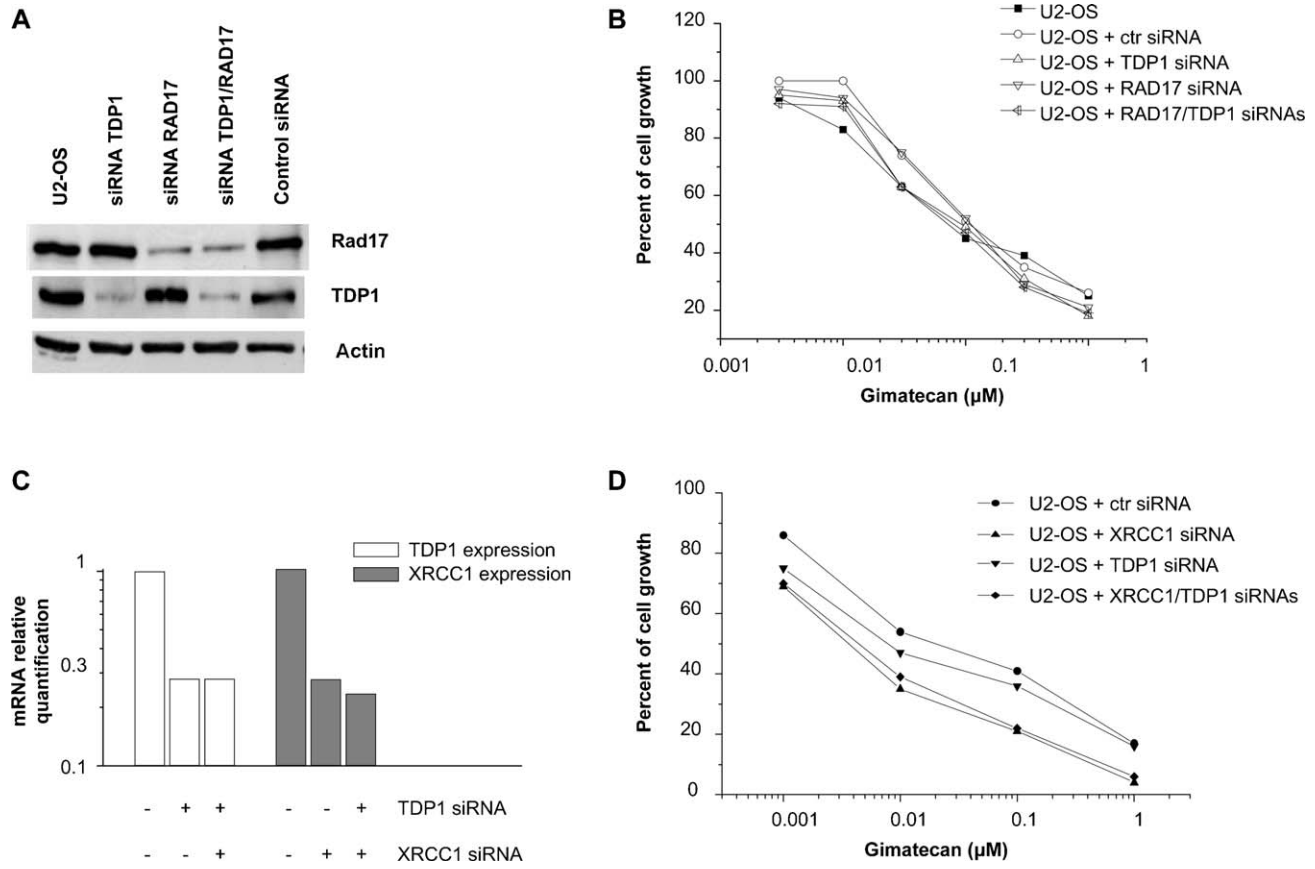

Fig. 3. RAD17, XRCC1 and TDP1 loss of function studies in U2OS cells. (A) Western blot analysis of levels of TDP1 and Rad17 in U2-OS cells transfected with 100 nM TDP1 and 50 nM Rad17 siRNAs for 4 h and harvested 48 h later. Control loading is shown by β-actin. (B) Cell sensitivity to gimatecan of cells transfected as indicated in (A) measured 72 h after 1 h drug exposure using growth inhibition assay. (C) Real time PCR analysis of levels of TDP1 and XRCC1 in cells transfected with TDP1 and XRCC1 siRNAs harvested as in (A). (D) Cell sensitivity to gimatecan in cells transfeted with siRNAs to TDP1 or XRCC1 or both, as assessed by sulforhodamine B assay after 48 h drug exposure. Standard deviation is less than 5% for each point.

Analysis of SSBs levels after 1 h exposure to 0.3 μM gimatecan (drug concentration around IC_{80}) using the alkaline comet assay indicated the lack of a direct relationship between the levels of damage measured at the end of 1 h treatment and drug-induced inhibition of cell proliferation (Table S3).

Based on the role of BRCA1 in homologous recombination which participate to DNA repair [37], U2-OS cells expressing the TDP1-targeting miRNA were used to knock down the BRCA1 protein and to evaluate whether a cooperation exist between the two repair pathways. A marked reduced expression of BRCA1 was achieved (Fig. 4A). The silencing of BRCA1 protein resulted in increased sensitivity to gimatecan (Fig. 4B and Fig. S4) both in U2-OS cells (4-fold-ctr siRNA *versus* BRCA1siRNA) and in U2-OS miRNA ctr cells (6-fold-ctr siRNA *versus* BRCA1 siRNA). Moreover, hypersensitivity (14 fold-ctr siRNA *versus* BRCA1 siRNA) was observed when both TDP1 and BRCA1 were down modulated.

3.6. TDP1 overexpression in U2-OS cells

To further define the significance of TDP1 in relation to response to CPTs, U2-OS cells were stably transfected with the full-length TDP1 cDNA. The phenotypic characterization of the transfected cells using different methods, i.e., Real-time PCR, Western blot and immunofluorescence analysis confirmed the over-expression of TDP1 in the model system (Fig. 5A–C). When performing growth-inhibition assays, no significant changes in the IC_{50} values after exposure to CPT, TPT or gimatecan were found between cells transfected with the empty vector and TDP1 over-expressing cells (Fig. S5A). An analysis of the pattern of sensitivity to a number of antitumor agents with different mechanisms of actions (i.e., taxol, cisplatin – data not shown) indicated lack of substantial changes in the IC_{50} values, except than for doxorubicin and etoposide, two Topo II inhibitors (Fig. S5B). Moreover, we found that SSBs after 1 h exposure to gimatecan were reduced in TDP1 over-expressing cells as compared with empty-vector transfected cells, as shown by alkaline comet assay (Table S4). Indeed, the median tail moment of U2-OS/TDP1 cells was lower than that of empty vector-transfected cells in cells were exposed to 0.3 μM gimatecan, a concentration corresponding to the IC_{80}. The median tail moment of U2-OS/TDP1 cells treated with 0.3 μM drug was significantly different from that of empty-vector transfected cells exposed to the same concentration of Topo I inhibitor.

4. Discussion

The cell response to CPTs is a complex phenomenon which involves multiple pathways whose activity and function affect the ultimate fate after drug-induced stress. In this context, DNA repair acts to limit the persistence of drug-induced damage. DNA damage persistence represents an important aspect for the efficacy of CPTs, due to the reversible nature of the ternary complex (drug–enzyme–DNA). CPT analogues endowed with increased ability to induce Topo I-mediated DNA cleavage and more persistent stabilization of the ternary complex display increased cytotoxic potency and enhanced efficacy [26]. In

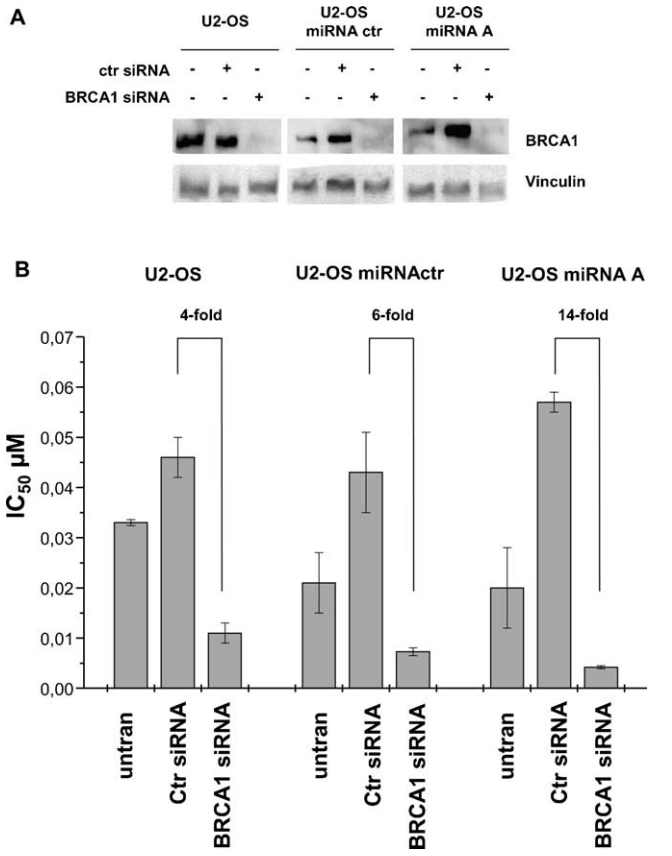

Fig. 4. Analyses of TDP1 and BRCA1 levels and cell sensitivity to gimatecan in TDP1 and BRCA1 co-silenced cells. (A) Western blot analysis of levels of BRCA1 in U2-OS cells expressing miRNA directed to TDP1 transfected with 100 nM BRCA1 siRNAs for 4 h and harvested 48 h later. Vinculin was used as control loading. (B) Cell sensitivity to gimatecan was determined using cell counter 72 h after 1 h exposure to gimatecan.

particular gimatecan, a lipophilic CPT currently undergoing Phase II clinical evaluation was found to induce persistent DNA damage [24].

The present study was originally designed with the aim of identifying cellular changes associated with resistance to gimatecan in an attempt to explore whether specific alterations may be targeted for modulation of CPT-based antitumor treatment. Whereas it has been documented that the expression of drug transporters can affect the efficacy of CPTs such as TPT and SN38, gimatecan has been shown to bypass defence mechanisms involving ABC transporters including Gp170, MRPs and BCRP [25,26]. In ovarian carcinoma cell lines generated *in vitro* by chronic exposure to the drug and thus exhibiting acquired resistance to gimatecan, we found increased expression of MRP2 but no change in gimatecan uptake. Worthy of note, we found that TDP1, but not TDP2, was a factor possibly implicated in cellular resistance, because increased protein levels were observed in two independently selected resistant cell systems as compared with parental cells. Such a feature was associated with a reduced sensitivity to two different TDP1 inhibitors observed in the resistant variants and with their enhanced capability to repair SSBs, as documented by alkaline elution. Thus, our cell model may be useful to set up an assay to identify TDP1 targeting compounds capable of improving the damage produced by CPTs at pharmacologically relevant concentrations. In addition, the related *in vivo* model could be useful in investigating strategies of drug combination aimed at overcoming CPT-resistance.

Although multiple molecular pathways are implicated in the repair of Topo I-mediated DNA damage induced by CPTs, TDP1 plays a peculiar role because it acts to repair DNA encumbered with the protein adduct in which Topo I is linked to a broken DNA end through a 3′ phosphoryl group [38]. Thus, the enzyme may be regarded to as a modulation target because its inhibition is expected to enhance the cellular activity of Topo I poisons.

In an attempt to clarify the interest of TDP1 as a putative target to improve the efficacy of gimatecan, we used the U2-OS cell line that can be engineered more easily than the ovarian carcinoma cell line employed in our study. Using loss and gain of function approaches (i.e., RNA interference and over-expression of TDP1 full-length DNA), we demonstrated that TDP1 *per se* cannot account for high levels of resistance to gimatecan. Indeed, upon gene silencing in U2-OS cells transiently transfected with synthetic siRNAs or stably expressing an exogenous miRNA targeting TDP1, we could not observe an increased sensitivity to the drug. This observation is consistent with similar levels of SSBs in cells transfected with control or TDP1 siRNAs. The lack of a substantial change in cell sensitivity after knocking-down TDP1 with two different approaches is in keeping with observations in fission yeast, in which deletion of the TDP1 gene is not sufficient to cause hypersensitivity to CPT [36]. In contrast, increased sensitivity to the drug can be reached when simultaneously deleting genes belonging to additional pathways, such as checkpoint control [36]. Thus, we used siRNA approach with the intent of clarifying the role of different factors eventually cooperating with TDP1 in drug resistance to CPTs. In this regard, the factors to be silenced together with TDP1 were chosen on the basis of physical or functional interaction reported in the literature.

In our model system, the concomitant silencing of TDP1 and the checkpoint control gene Rad17 produced only a slight change in cell sensitivity, suggesting that in human cells the pathways for repairing Topo I-mediated damage are redundant and some of them cooperate in limiting CPT-induced damage. In fact, although it is possible that simultaneous knocking-down of these two genes causes an increase in the levels of damage due to the role of RAD17 in a checkpoint that stabilizes arrested replication forks [39], a relevant change in cell sensitivity was not found.

In the osteosarcoma cells, the silencing of XRCC1 or BRCA1 produced an increase in sensitivity to gimatecan. An improvement in cell sensitivity was observed after the knockdown of both TDP1 and BRCA1. This observation suggests that the repair process may mainly rely on XRCC1 or BRCA1 and that, under our conditions, TDP1 alone may appear dispensable. The effects of the inactivation of the examined pathways in regulation sensitivity to CPTs are not obvious. In fact, although a role for homologous recombination in repair of gimatecan damage is reasonable, BRCA1 knockdown confers hypersensitivity to gimatecan, whereas BRCA2 does not (data not shown). A role for BRCA1 was also supported by the increase in its levels observed in gimatecan-resistant cells, particularly in IGROV-1CPT/L.

The role of TDP1 may be dependent on the cellular context because a coordinated regulation of XRCC1 and TDP1 has been reported [40]. Indeed, transfection of TDP1 in XRCC1 deficient cells, which are hypersensitive to CPT, results in increased activity of TDP1 [40]. However, in our model system, no changes in TDP1 levels were found as a consequence of XRCC1 inactivation as assessed by Western blot experiments (data not shown). Moreover, although inhibition of PARP1 enzyme activity has been reported to interfere with DNA Base Excision Repair and to sensitize cells to apoptotic stimuli [41], no change in cellular sensitivity to gimatecan was observed in osteosarcoma cells silenced for TDP1 and overexpressing PARP1 dominant negative. This result indicates, at least in our cell system, an absence of cooperation between two enzymes of the same repair pathway.

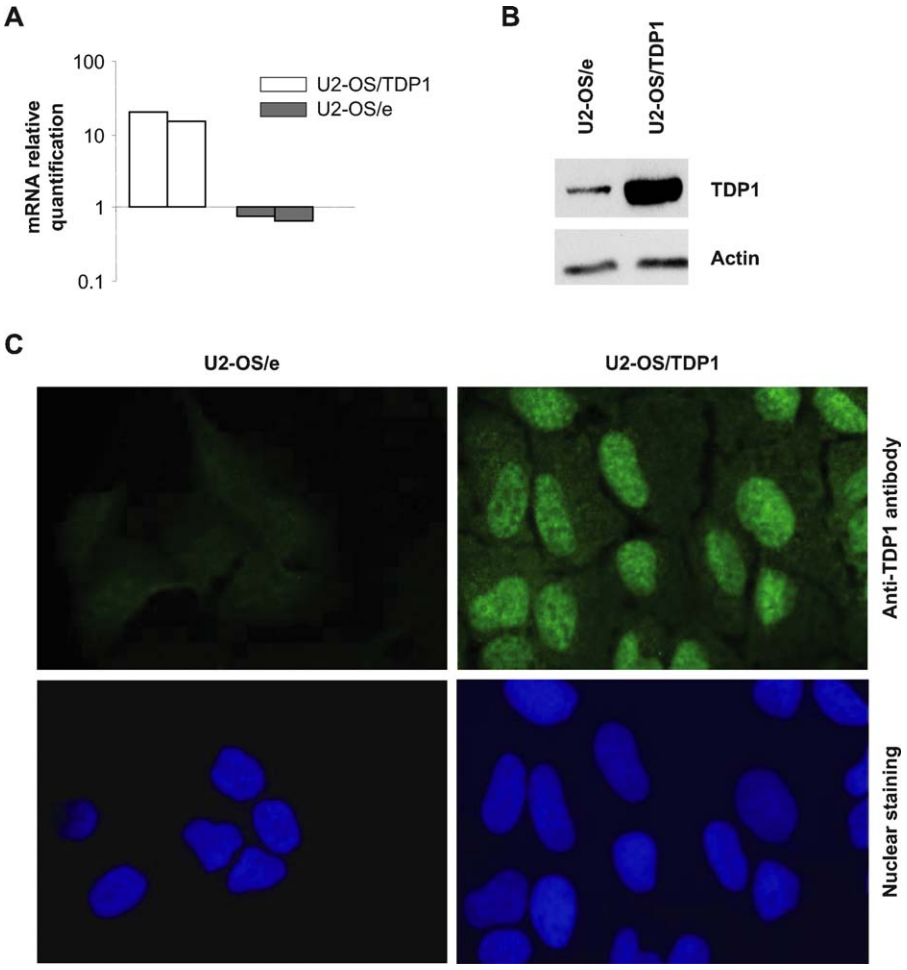

Fig. 5. Analyses of TDP1 levels in TDP1 cDNA U2-OS transfected cells. Real time PCR (A), Western blot (B) and immunofluorescence analysis (C) of TDP1 levels in U2-OS cell transfected with pDEST12.2 containing TDP1 full length cDNA (U2-OS/TDP1) or pDEST12.2 empty vector (U2-OS/e). (A) The two columns for each cell line represent 2 independent experiments; TDP1 transcript levels were normalized to GAPDH and referred to the untransfected cells; (B) control loading is shown by β-actin; (C) cells were stained for TDP1 and nuclei were counterstained with Heochst33342.

Our results suggest that redundant pathways act to limit Topo I mediated damage. The redundancy of the pathways implicated in repair of Topo I-mediated damage is also documented by the analysis of sensitivity to gimatecan of TDP1 over-expressing cells. In fact, a small increase in IC_{50} (1.6 fold) was observed in U2-OS-TDP1 cells, when using a cell survival assay (i.e., colony-forming assay, data not shown). Such a modulation is of the same magnitude of that reported in cells infected with retroviral vector encoding for TDP1 [42]. Although over-expression of TDP1 in U2-OS cells did not result in acquisition of significant levels of resistance, a reduced level of SSBs was documented in these cells as compared with cells transfected with the empty vector. In summary, our results indicate that TDP1 contributes in part to resistance to gimatecan as suggested by increased expression in resistant cells and by reduced levels of damage in cells transfected with TDP1 full-lenght cDNA. However, TDP1 alone cannot account for relevant levels of resistance as shown by loss and gain of function approaches. Such results are in keeping with studies with knock-out mice showing that TDP1 facilitates SSB repair in primary neural cells [43]. The cooperation between TDP1 and other pathways in regulating sensitivity to CPTs is a realistic event, but the critical players of gimatecan induced damage do not act synergistically with TDP1.

In conclusion, since TDP1 alone can account for mild levels of camptothecin resistance, repair of Topo I mediated damage likely occur through redundant pathways mainly implicating BRCA1 and XRCC1, but not RAD17 and PARP1. These findings may be relevant to define novel therapeutic strategies.

Conflict of interest

All authors disclose any actual or potential conflict of interest.

Acknowledgments

We thank Dr. Loana Musso for technical support. This work was supported by the Associazione Italiana per la Ricerca sul Cancro, Milan and by the Ministero della Salute, Rome, Italy.

Appendix A. Supplementary data

Supplementary data associated with this article can be found, in the online version, at doi:10.1016/j.bcp.2011.09.021.

References

[1] Wang JC. DNA topos. Annu Rev Biochem 1996;65:635–92.
[2] Pommier Y, Pourquier P, Fan Y, Strumberg D. Mechanism of action of eukaryotic DNA Topo I and drugs targeted to the enzyme. Biochim Biophys Acta 1998;1400:83–105.

[3] Pizzolato JF, Saltz LB. The camptothecins. Lancet 2002;361:2235–42.
[4] Zunino F, Pratesi G. Camptothecins in clinical development. Exp Opin Investig Drugs 2004;13:269–84.
[5] Rasheed ZA, Rubin EH. Mechanisms of resistance to Topo I-targeting drugs. Oncogene 2003;22:7296–304.
[6] Beretta GL, Perego P, Zunino F. Mechanisms of cellular resistance to camptothecins. Curr Med Chem 2006;13:3291–305.
[7] Ambudkar SV, Kimchi-Sarfaty C, Sauna ZE, Gottesman MM. P-glycoprotein: from genomics to mechanism. Oncogene 2003;22:7468–85.
[8] Maliepaard M, van Gastelen MA, de Jong LA, Pluim D, van Waardenburg RC, Ruevekamp-Helmers MC, et al. Overexpression of the BCRP/MXR/ABCP gene in a topotecan-selected ovarian tumor cell line. Cancer Res 1999;59:4559–63.
[9] Allen JD, Brinkhuis RF, Wijnholds J, Schinkel AH. The mouse Bcrp1/Mxr/Abcp gene: amplification and overexpression in cell lines selected for resistance to topotecan, mitoxantrone, or doxorubicin. Cancer Res 1999;59:4237–41.
[10] Leggas M, Adachi M, Scheffer GL, Sun D, Wielinga P, Du G, et al. Mrp4 confers resistance to topotecan and protects the brain from chemotherapy. Mol Cell Biol 2004;24:7612–21.
[11] Gatti L, Beretta GL, Cossa G, Zunino F, Perego P. ABC transporters as potential targets for modulation of drug resistance. Mini Rev Med Chem 2009;9:1102–12.
[12] Wang LF, Ting CY, Lo CK, Su JS, Mickley LA, Fojo AT, et al. Identification of mutations at DNA Topo I responsible for camptothecin resistance. Cancer Res 1997;57:1516–22.
[13] Tsurutani J, Nitta T, Hirashima T, Komiya T, Uejima H, Tada H, et al. Point mutations in the Topo I gene in patients with non-small cell lung cancer treated with irinotecan. Lung Cancer 2002;35:299–304.
[14] Redinbo MR, Stewart L, Kuhn P, Champoux JJ, Hol WG. Crystal structures of human Topo I in covalent and noncovalent complexes with DNA. Science 1998;279:1504–13.
[15] Desai SD, Li TK, Rodriguez-Bauman A, Rubin EH, Liu LF. Ubiquitin/26S proteasome-mediated degradation of Topo I as a resistance mechanism to camptothecin in tumor cells. Cancer Res 2001;61:5926–32.
[16] Horie K, Tomida A, Sugimoto Y, Yasugi T, Yoshikawa H, Taketani Y, et al. SUMO-1 conjugation to intact DNA Topo I amplifies cleavable complex formation induced by camptothecin. Oncogene 2002;21:7913–22.
[17] Zhang Y, Fujita N, Tsuruo T. p21Waf1/Cip1 acts in synergy with bcl-2 to confer multidrug resistance in a camptothecin-selected human lung-cancer cell line. Int J Cancer 1999;83:790–7.
[18] Fujimori A, Gupta M, Hoki Y, Pommier Y. Acquired camptothecin resistance of human breast cancer MCF-7/C4 cells with normal topo I and elevated DNA repair. Mol Pharmacol 1996;50:1472–8.
[19] Park SY, Lam W, Cheng YC. X-ray repair cross-complementing gene I protein plays an important role in camptothecin resistance. Cancer Res 2002;62:459–65.
[20] Barthelmes HU, Habermeyer M, Christensen MO, Mielke C, Interthal H, Pouliot JJ, et al. TDP1 overexpression in human cells counteracts DNA damage mediated by topoisomerases. I and II. J Biol Chem 2004;279:55618–25.
[21] Das BB, Dexheimer TS, Maddali K, Pommier Y. Role of tyrosyl-DNA phosphodiesterase (TDP1) in mitochondria. Proc Natl Acad Sci USA 2010;107:19790–5.
[22] Zeng Z, Cortes-Ledesma F, El-Khamisy SF, Caldecott KW. TDP2/TTRAP is the major 5′-tyrosyl DNA phosphodiesterase activity in vertebrate cells and is critical for cellular resistance to topoisomerase II-induced DNA damage. J Biol Chem 2010;286:403–9.
[23] Cortes Ledesma F, El Khamisy SF, Zuma MC, Osborn K, Caldecott KW. A human 5′-tyrosyl DNA phosphodiesterase that repairs topoisomerase-mediated DNA damage. Nature 2009;461:674–8.
[24] Dallavalle S, Ferrari A, Biasotti B, Merlini L, Penco S, Gallo G, et al. Novel 7-oxyiminomethyl derivatives of camptothecin with potent *in vitro* and *in vivo* antitumor activity. J Med Chem 2001;44:3264–74.
[25] De Cesare M, Pratesi G, Perego P, Carenini N, Tinelli S, Merlini L, et al. Potent antitumor activity and improved pharmacological profile of ST1481, a novel 7-substituted camptothecin. Cancer Res 2001;61:7189–95.
[26] Perego P, De Cesare M, De Isabella P, Carenini N, Beggiolin G, Pezzoni G, et al. A novel 7-modified camptothecin analog overcomes breast cancer resistance protein-associated resistance in a mitoxantrone-selected colon carcinoma cell line. Cancer Res 2001;61:6034–7.
[27] Perego P, Romanelli S, Carenini N, Magnani I, Leone R, Bonetti A, et al. Ovarian cancer cisplatin-resistant cell lines: multiple changes including collateral sensitivity to Taxol. Ann Oncol 1998;9:423–30.
[28] Perego P, Beretta GL, Gatti L. Identification of determinants of sensitivity to antitumor drugs. In: Conn PM, editor. Handbook of proteomic methods. Humana Press; 2002. p. 319–30.
[29] Buscemi G, Perego P, Carenini N, Nakanishi M, Chessa L, Chen J, et al. Activation of ATM and Chk2 kinases in relation to the amount of DNA strand breaks. Oncogene 2004;23:7691–700.
[30] Gatti L, Supino R, Perego P, Pavesi R, Caserini C, Carenini N, et al. Apoptosis and growth arrest induced by platinum compounds in U2-OS cells reflect a specific DNA damage recognition associated with a different p53-mediated response. Cell Death Differ 2002;9:1352–9.
[31] Pouliot JJ, Yao KC, Robertson CA. Nash HA Yeast gene for a Tyr–DNA phosphodiesterase that repairs Topo I covalent complexes. Science 1999;286:552–5.
[32] Interthal H, Pouliot JJ, Champoux JJ. The tyrosyl-DNA phosphodiesterase Tdp1 is a member of the phospholipase D superfamily. Proc Natl Acad Sci USA 2001;98:12009–14.
[33] Weidlich IE, Dexheimer T, Marchand C, Antony S, Pommier Y, Nicklaus MC. Inhibitors of human tyrosyl-DNA phospodiesterase (hTdp1) developed by virtual screening using ligand-based pharmacophores. Bioorg Med Chem 2010;18:182–9.
[34] Küpper JH, de Murcia G, Bürkle A. Inhibition of poly(ADP-ribosyl)ation by overexpressing the poly(ADP-ribose) polymerase DNA-binding domain in mammalian cells. J Biol Chem 1990;265:18721–4.
[35] Hans MA, Müller M, Meyer-Ficca M, Bürkle A, Küpper J. Overexpression of dominant negative PARP interferes with tumor formation of HeLa cells in nude mice: evidence for increased tumor cell apoptosis *in vivo*. Oncogene 1999;18:7010–5.
[36] Vance JR, Wilson TE. Yeast Tdp1 and Rad1-Rad10 function as redundant pathways for repairing Top1 replicative damage. Proc Natl Acad Sci USA 2002;99:13669–74.
[37] Wu J, Lu LY, Yu X. The role of BRCA1 in DNA damage response. Protein Cell 2010;1:117–23.
[38] El-Khamisy SF, Saifin GM, Weinfeld M, Johansson F, Helleday T, Lupski JR, et al. Defective DNA single-strand break repair in spinocerebellar ataxia with axonal neuropathy-1. Nature 2005;434:108–13.
[39] Budzowska M, Kanaar R. Mechanisms of dealing with DNA damage-induced replication problems. Cell Biochem Biophys 2009;53:17–31.
[40] Plo I, Liao ZY, Barceló JM, Kohlhagen G, Caldecott KW, Weinfeld M, et al. Association of XRCC1 and tyrosyl DNA phosphodiesterase (Tdp1) for the repair of topoisomerase I-mediated DNA lesions. DNA Repair 2003;2:1087–100.
[41] Pommier Y, Barcelo JM, Rao VA, Sordet O, Jobson AG, Thibaut L, et al. Repair of topoisomerase I-mediated DNA damage. Prog Nucleic Acid Res Mol Biol 2006;81:179–229.
[42] Nivens MC, Felder T, Galloway AH, Pena MM, Pouliot JJ, Spencer HT. Engineered resistance to camptothecin and antifolates by retroviral coexpression of tyrosyl DNA phosphodiesterase-I and thymidylate synthase. Cancer Chemother Pharmacol 2004;53:107–15.
[43] Katyal S, el-Khamisy SF, Russell HR, Li Y, Ju L, Caldecott KW, et al. TDP1 facilitates chromosomal single-strand break repair in neurons and is neuroprotective *in vivo*. EMBO J 2007;26:4720–31.